Time-Resolved Powder X-ray Diffraction of the Solvothermal Crystallization of Cobalt Gallate Spinel Photocatalyst Reveals Transient Layered Double Hydroxides

Cook, Daniel S ; Wu, Yue ; Lienau, Karla ; Moré, René ; Kashtiban, Reza J ; Magdysyuk, Oxana V ; Patzke, Greta R ; Walton, Richard I

DOI: https://doi.org/10.1021/acs.chemmater.7b01761

CHEMISTRY OF MATERIALS

Communication

pubs.acs.org/cm

Time-Resolved Powder X-ray Diffraction of the Solvothermal Crystallization of Cobalt Gallate Spinel Photocatalyst Reveals Transient Layered Double Hydroxides

Daniel S. Cook,[†] Yue Wu,[‡] Karla Lienau,[§] René Moré,[§] Reza J. Kashtiban,[∥] Oxana V. Magdysyuk,[⊥] Greta R. Patzke,[§] and Richard I. Walton*[,†]

[†]Department of Chemistry, University of Warwick, Coventry CV4 7AL, United Kingdom

[‡]Department of Materials Science & Metallurgy, University of Cambridge, 27 Charles Babbage Road, Cambridge CB3 0FS, United Kingdom

[§]Department of Chemistry, University of Zurich, Winterthurerstrasse 190, CH-8057 Zurich, Switzerland

[∥]Department of Physics, University of Warwick, Coventry CV4 7AL, United Kingdom

[⊥]Diamond Light Source Ltd., Harwell Science and Innovation Campus, Didcot Ox11 0DE, United Kingdom

Supporting Information

Spinel oxides are an important family of materials studied for their electronic and magnetic properties and find use in many functional applications,[1] in particular catalysis[2] and photocatalysis.[3,4] The metal deficient spinel γ-Ga_2O_3 has been applied for the photocatalytic degradation of volatile aromatics[5] and mixed-metal gallium oxide spinels, such as $ZnGa_2O_4$, have been employed for the photocatalytic degradation of organic pollutants.[6] The high temperatures required for the synthesis of many oxides usually prohibit the study of the mechanisms and reaction pathways of their formation. Such knowledge would be highly desirable to predict the outcome of future synthesis so to tailor materials with useful properties. Moorhouse et al. recently reported a time-resolved *in situ* powder X-ray diffraction (XRD) study of $Bi_5Ti_3Fe_{0.5}Cr_{0.5}O_{15}$ crystallization from a molten salt reaction using high energy X-rays.[7] The high-quality data obtained from the synchrotron experiment allowed for full structural refinements to be undertaken on a host of metastable materials observed during the reaction. Developments in *in situ* methodologies for following crystallization have been the focus of extensive review articles and with state-of-the-art methodologies temporal evolution of crystalline structure, including phase fraction, lattice parameters and, in favorable cases, atomic-scale crystal structure can be tracked.[8−11] In general, however, there are fewer reports on the *in situ* study of crystallization of dense oxide materials,[12−15] compared to the growing body of data on the formation of open-framework zeolites and metal−organic frameworks.[16,17] We herein report the use of *in situ* X-ray diffraction to study the solvothermal crystallization of a gallium oxide spinel material.

The solvothermal synthesis of γ-Ga_2O_3 can be effected directly from gallium metal in an aminoalcohol solvent.[18,19] Mixed-metal spinels can be prepared by the same route if a transition metal salt (e.g., of Co, Ni, Fe or Zn) is introduced into the solution.[20] The material $Co_{0.973(8)}Ga_{1.767(8)}O_{3.752(8)}$ produced by this method was shown to be a largely inverse spinel (i.e., a mixture of both Co^{2+} and Ga^{3+} on both tetrahedral and octahedral sites) with a composition and inversion parameter different to cobalt gallium oxides synthesized at high temperature, although typically having a similar composition of $CoGa_2O_4$.[21,22] To understand the formation mechanism of this spinel, time-resolved XRD experiments were carried out using the Oxford-Diamond *In Situ* Cell (ODISC)[23] on beamline I12 at the Diamond Light Source, UK,[24] that makes use of a large image plate detector to allow powder diffraction patterns to be taken in a few seconds with excellent *d*-spacing resolution. The use of high energy X-rays (~65.6 keV) allows penetration of the steel autoclave and polytetrafluoroethylene (PTFE) liner. The advantage of this setup is the large volume (25 mL) reactor that mimics real laboratory synthesis conditions, and while data quality is limited by background scatter, the measured patterns do provide quantitative information, such as lattice parameters of materials present. Two experiments are presented herein: the spinel formation in a water-monoethanolamine (MEA) mixture and the formation in only MEA. The photocatalytic properties of the spinels synthesized from both reaction conditions are then presented.

In the reaction of gallium metal and cobalt(II) nitrate hexahydrate (2:1 ratio) in monoethanolamine (MEA) and water mixture (1:1 by volume) at 210 °C, transient phases with complex growth and decay profiles precede the formation of the expected cobalt gallium oxide (Figure 1a). The first period of growth and decay of the transients can be seen to occur within the first 45 min of reaction (Figure 1b) with a decreased *d*-spacing of its Bragg reflections (i.e., a shift to higher diffraction angle). The Bragg reflections of a transient phase increase in intensity again, and reach a second maximum intensity at around 120 min. A second decay period occurs without reaching a plateau and almost immediately with the onset of spinel growth, suggesting that the onset of spinel growth and decay of the transient phase are closely related. At 450 min, the intensity of the spinel oxide phase begins to plateau whereas the transient phase intensity has almost disappeared, which together indicate that the reaction is

Received: May 2, 2017
Revised: June 6, 2017
Published: June 6, 2017

DOI: 10.1021/acs.chemmater.7b01761
Chem. Mater. 2017, 29, 5053−5057

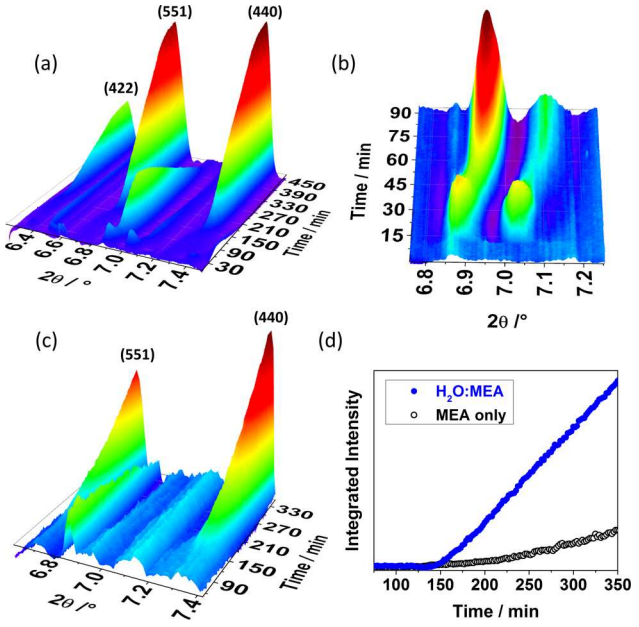

Figure 1. (a) Contour map of the higher angle peaks of the *in situ* experiment (λ = 0.18893 Å) with MEA:H_2O as solvent with Miller indices of spinel product labeled, (b) close-up of the contour map showing the emergence of the transient phase after around 15 min with rapid decay before a slower secondary period of growth occurs, (c) contour map of the higher angle peaks when MEA only is used as solvent with Miller indices of spinel product labeled and (d) comparison of crystallization curves.

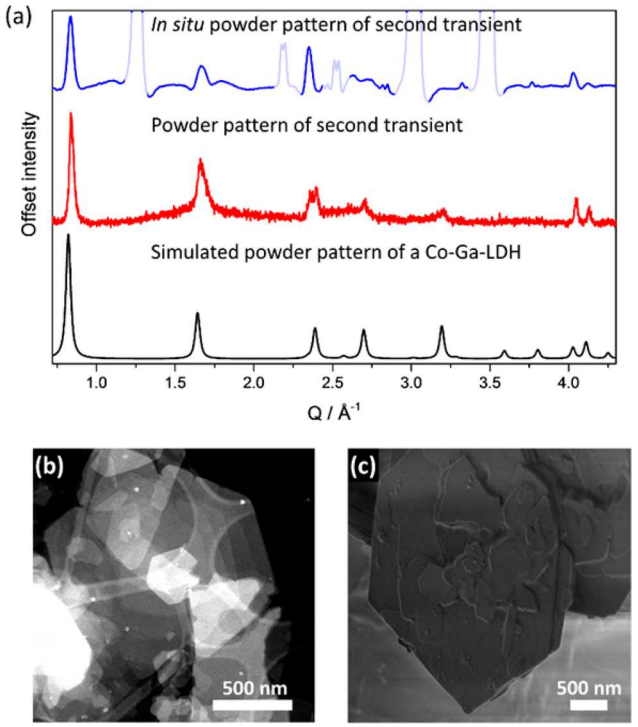

Figure 2. (a) PXRD patterns of a simulated Co-Ga-LDH (black), isolated second transient Co-Ga-LDH (red) and from the formation of Co-Ga-LDH *in situ* (blue). Faded peaks are steel autoclave and PTFE; background was subtracted using the rolling-ball method. (b) ADF-STEM image of isolated Co-Ga-LDH showing large hexagonal plate morphology. (c) SEM image showing similar hexagonal plate morphology.

coming to completion. A similar reaction conducted using solely MEA as the solvent also formed a cobalt gallium oxide spinel with onset of crystallization after around 150−175 min. However, in this case there was no formation of any crystalline intermediate (Figure 1c). Though the onset of spinel growth occurs at a similar time, the rate at which the spinel grows in MEA only is much slower than in the reaction containing a mixture of MEA and water (Figure 1d). The difference in the rate of spinel growth could be attributed to the greater viscosity of the organic solvent,[25] which might affect either (or both) diffusion of reagents in solution or stirring rate, rather than necessarily being directly related to the formation of the intermediate seen when water is present.

Off-line experiments with ODISC were used to attempt to isolate the transient phase(s). The powder X-ray diffraction (PXRD) pattern of the isolated solid after approximately 80 min is in good agreement with the *in situ* data after the same reaction time (the second transient phase, Figure 2a). Indexing and Pawley refinement yielded a rhombohedral cell, (space group $R\bar{3}m$), with lattice parameters (hexagonal setting) of a = 3.111(2) Å, c = 22.65(3) Å, which are characteristic of a layered double hydroxide (LDH). Indeed, the refined parameters are very similar to those reported for Co−Ga LDHs in the literature.[26,27] A further, shorter offline experiment aimed at isolating the first transient phase gave an LDH (present among other unidentified material(s)) that has a larger unit cell than the second LDH (see Figure S4), in agreement with the shift in d-spacing of the diffraction data observed *in situ*. Electron microscopy showed that the morphology of the first isolated phase consists of thin hexagonal plates (Figure 2b,c), typical of an LDH,[28,29] whereas EELS (TEM) and EDX (SEM) suggests the presence of Co and Ga in a ratio of 1:1.

This ratio is different from that of the final product, suggesting that the LDH does not directly convert into the spinel through a solid−solid transformation. TGA-DSC coupled with mass spectrometry proved the presence of occluded water and nitrate in the LDH interlayer gallery. Therefore, a possible empirical formula of the isolated LDH is $[(Co_{0.5}Ga_{0.5})(OH)_2](NO_3)_{0.5}{\cdot}xH_2O$, assuming the presence of only Co^{2+}. It has been established that synthetic LDHs can be formed with a higher M^{3+} content than in natural minerals,[30−34] and although this composition has not previously been reported for a Co-Ga-LDH, it is not chemically unreasonable. While the powder XRD shows the presence of no crystalline impurities, and no obvious impurity phase was seen by TEM, we cannot rule out the presence of small amounts of amorphous M(III) hydroxides or Ga metal, although the uniform color of the isolated LDH would suggest that levels of impurities are small. With an identification of the second transient phase, and the similarity of its diffraction pattern to that of the first transient phase also suggesting a layered hydroxide, the integrated intensities of the most intense peaks of each phase were determined to provide a graphical representation of the extent of reaction, plotted as α, the peak intensity normalized to its maximum value (Figure 3a).

The growth of the first LDH commences around 15 min, after the autoclave stabilized at 210 °C (Figure 3b) so the subsequent events are under isothermal conditions. The decay of the second LDH and spinel growth do not cross at α = 0.5 (Figure 3a), which provides evidence that the LDH is not evolving directly into the spinel, but most likely dissolves to give a solution that contains the correct ratio of metals from

DOI: 10.1021/acs.chemmater.7b01761
Chem. Mater. 2017, 29, 5053−5057

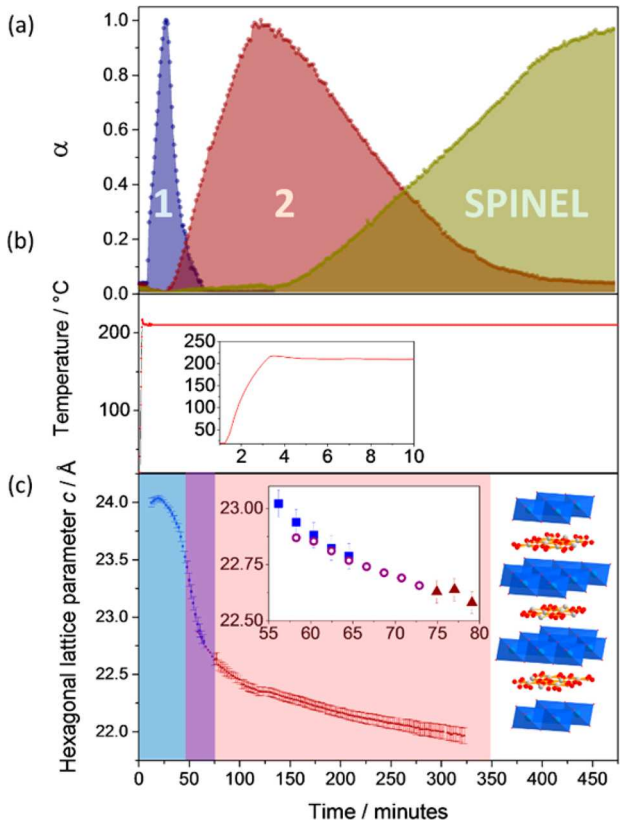

Figure 3. (a) Reaction overview from integrated intensities of LDH and spinel Bragg peaks, (b) plot of temperature of reactor, (c) evolution of the LDH *c* lattice parameter as a function of time with (inset) blue squares representing the 1st LDH, mauve circles the 2nd LDH coexisting with the 1st LDH, and maroon triangles the 2nd LDH after disappearance of the 1st LDH together with a schematic structure of the LDH.

which the spinel crystallizes. Given the difference in structures of the LDH (edge-shared hydroxide octahedra) and the spinel (close-packed oxide with octahedral and tetrahedral metals) a direct solid transformation is not expected. Indeed, the thermal transformation of LDHs into spinels, even when the metal ratios are maintained, usually occur via phase separation into binary oxides or amorphous materials.[35]

Sequential Pawley refinements show that the *c* lattice parameter rapidly shrinks during the first growth and decay period of the LDH.[36] The *c* parameter continues to shrink in size albeit at a slower rate during both the secondary growth and decay. After 325 min, only a small amount of LDH remains and further refinements were not possible (Figure 3c). A likely explanation of the continuous contraction of the *c* parameter is loss of interlayer water molecules (Figure 3c inset), whereas reorientation of the interlayer nitrate or water might also be a possible reason.[37] Further confirmation of the anisotropic structure is provided by the much smaller evolution of (*hk*0) reflection positions compared to (00*l*) reflection positions (see Figure S6).

PXRD of spinels from both reactions (Figure 4) reveals that the reaction in ethanolamine and water formed a spinel that was much more crystalline than that made in ethanolamine alone.

Lattice parameters for the spinel formed in H_2O:MEA mixture and ethanolamine were refined to a = 8.3257(3) Å, and a = 8.3302(15) Å, respectively. The larger cell for the less

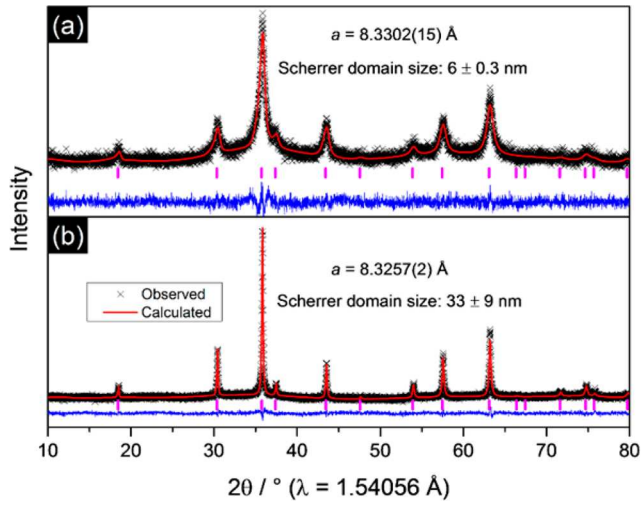

Figure 4. Pawley fits to PXRD data (Cu Kα_1) for (a) spinel made in MEA only (b) for spinel made in 1:1 H_2O:MEA.

crystalline sample is consistent with an expansion of the unit cell due to nanosized crystal domains.

Despite the smaller crystallite domains in the sample made in strictly solvothermal conditions, the BET surface areas of the two materials are virtually the same; this is explained by the fact that the sample prepared in MEA alone consists of highly agglomerated nanodomains, as shown by high resolution TEM (see Figure S12).

We studied the photocatalytic properties of the cobalt gallium oxide spinels by investigating their use as water oxidation catalysts by the well-established *tris*(bipyridine)-ruthenium(II)–sodium persulfate system.[38,39] Labeling experiments proved water to be the source of the produced oxygen and PXRD after catalysis revealed the stability of the material (see Figure S15). ICP-MS analyses indicated only minor leaching of Co and Ga during catalysis from the photocatalyst synthesized in 1:1 H_2O:MEA, while more significant leaching of 2.85% Ga was observed in the catalyst synthesized in MEA, pointing to its lower stability. Table 1 summarizes the results,

Table 1. Characterisation and Photocatalysis Results from $CoGa_2O_4$ Spinels, along with a Co_3O_4 Reference Material

Material	BET surface area ($m^2\ g^{-1}$)	O_2 (μmol)	% Yield O_2 relative to $Na_2S_2O_8$	μmol O_2 (m^2)
$CoGa_2O_4$ (MEA)	30	4.7 ± 0.2	23.3 ± 0.8	94.3 ± 12.6
$CoGa_2O_4$ (MEA:H_2O)	32	6.0 ± 1.1	30.1 ± 4	77.8 ± 2.8
Co_3O_4 (commercial)	36	2.5 ± 0.3	12.7 ± 1.6	34.7 ± 4.5
Co_3O_4 (microwave)	26	6.1 ± 1.1	30.6 ± 5.3	135.1 ± 9.9

along with surface normalization. The new $CoGa_2O_4$ materials have similar activities to each other, but the surface-normalized activity is apparently lower than the microwave-synthesized Co_3O_4 reference (also a spinel of similar surface area). This difference in activity might arise from the presence of a lower concentration of surface cobalt in the mixed-metal materials than in the Co_3O_4 reference. Furthermore, Co_3O_4 contains a mixture of Co^{2+} and catalytically active Co^{3+},[40,41] unlike the gallate spinels that contain mainly Co^{2+}, which may also

DOI: 10.1021/acs.chemmater.7b01761
Chem. Mater. 2017, 29, 5053−5057

account for the differences observed. The catalysis is clearly very sensitive to the surface chemistry, because upon annealing the activity is completely removed.

It is relevant to note that spinels are often prepared by firing layered double hydroxides at high temperatures (300−500 °C).[42−44] Our work shows that these layered hydroxides can form *in situ* in solution as metastable phases followed by redissolution into the solvent, or amorphization, before formation of the spinel oxide. The fast acquisition time of the *in situ* XRD uniquely allowed for observation of two transient phases including one in particular which is very short-lived and unlikely to have been quenched and seen by conventional laboratory techniques. This work shows the complexity of solvothermal reactions, with the transient presence of kinetically stable products meaning that predicting the outcome of exploratory synthesis for the discovery of new functional materials remains extremely challenging.

■ ASSOCIATED CONTENT

Supporting Information

The Supporting Information is available free of charge on the ACS Publications website at DOI: 10.1021/acs.chemmater.7b01761.

Full details of the analysis of the *in situ* PXRD, thermogravimetry, XANES, characterization of materials and details of photocatalysis. (PDF)

■ AUTHOR INFORMATION

Corresponding Author

*Richard I. Walton. E-mail: r.i.walton@warwick.ac.uk.

ORCID

Richard I. Walton: 0000-0001-9706-2774

Notes

The authors declare no competing financial interest.

■ ACKNOWLEDGMENTS

D.S.C. thanks the EPSRC for the award of a CASE studentship. K.L., R.M., and G.R.P. thank the UZH research priority program "Light to Chemical Energy Conversion" (URPP LightChEC) for financial support. G.R.P. thanks the Swiss National Science Foundation (Sinergia Grant No. CRSII2_160801/1) for financial support. We thank Diamond Light Source for provision of beamtime (EE12884). We are grateful to Mr. David Hammond for the TGA analysis and Mr. Alexander Dunn for assistance with SEM. The research data supporting this publication can be accessed at: http://wrap.warwick.ac.uk/88999.

■ REFERENCES

(1) Grimes, N. W. The Spinels: Versatile Materials. *Phys. Technol.* **1975**, *6*, 22−27.

(2) Wachs, I. E.; Routray, K. Catalysis Science of Bulk Mixed Oxides. *ACS Catal.* **2012**, *2*, 1235−1246.

(3) Conrad, F.; Zhou, Y.; Yulikov, M.; Hametner, K.; Weyeneth, S.; Jeschke, G.; Günther, D.; Grunwaldt, J. D.; Patzke, G. R. Microwave-Hydrothermal Synthesis of Nanostructured Zinc-Copper Gallates. *Eur. J. Inorg. Chem.* **2010**, *2010*, 2036−2043.

(4) Conrad, F.; Bauer, M.; Sheptyakov, D.; Weyeneth, S.; Jaeger, D.; Hametner, K.; Car, P.-E.; Patscheider, J.; Günther, D.; Patzke, G. R. New Spinel Oxide Catalysts for Visible-Light-Driven Water Oxidation. *RSC Adv.* **2012**, *2*, 3076−3082.

(5) Hou, Y.; Wu, L.; Wang, X.; Ding, Z.; Li, Z.; Fu, X. Photocatalytic Performance of α-, β-, and γ-Ga_2O_3 for the Destruction of Volatile Aromatic Pollutants in Air. *J. Catal.* **2007**, *250*, 12−18.

(6) Anchieta, C. G.; Sallet, D.; Foletto, E. L.; Da Silva, S. S.; Chiavone-Filho, O.; Do Nascimento, C. A. O. Synthesis of Ternary Zinc Spinel Oxides and Their Application in the Photodegradation of Organic Pollutant. *Ceram. Int.* **2014**, *40*, 4173−4178.

(7) Moorhouse, S. J.; Wu, Y.; Buckley, H. C.; O'Hare, D. Time-Resolved in Situ Powder X-Ray Diffraction Reveals the Mechanisms of Molten Salt Synthesis. *Chem. Commun.* **2016**, *52*, 13865−13868.

(8) Pienack, N.; Bensch, W. In-Situ Monitoring of the Formation of Crystalline Solids. *Angew. Chem., Int. Ed.* **2011**, *50*, 2014−2034.

(9) Jensen, K. M. Ø.; Tyrsted, C.; Bremholm, M.; Iversen, B. B. In Situ Studies of Solvothermal Synthesis of Energy Materials. *ChemSusChem* **2014**, *7*, 1594−1611.

(10) Bøjesen, E. D.; Iversen, B. B. The Chemistry of Nucleation. *CrystEngComm* **2016**, *18*, 8332−8353.

(11) Walton, R. I.; Millange, F. In Situ Studies of the Crystallization of Metal−Organic Frameworks. In *The Chemistry of Metal−Organic Frameworks*; Kaskel, S., Ed.; Wiley-VCH Verlag GmbH & Co. KGaA, 2016; pp 729−764.

(12) Walton, R. I.; Millange, F.; Smith, R. I.; Hansen, T. C.; O'Hare, D. Real Time Observation of the Hydrothermal Crystallization of Barium Titanate Using in Situ Neutron Powder Diffraction. *J. Am. Chem. Soc.* **2001**, *123*, 12547−12555.

(13) Croker, D.; Loan, M.; Hodnett, B. K. Kinetics and Mechanisms of the Hydrothermal Crystallization of Calcium Titanate Species. *Cryst. Growth Des.* **2009**, *9*, 2207−2213.

(14) Zhou, Y.; Yuanhua, L.; Patzke, G. R. Synchrotron Radiation for the Study of Hydrothermal Formation Mechanisms of Oxide Nanomaterials. *Prog. Chem.* **2012**, *24*, 1583−1591.

(15) Philippot, G.; Boejesen, E. D.; Elissalde, C.; Maglione, M.; Aymonier, C.; Iversen, B. B. Insights into $BaTi_{1-y}Zr_yO_3$ ($0 \leq y \leq 1$) Synthesis under Supercritical Fluid Conditions. *Chem. Mater.* **2016**, *28*, 3391−3400.

(16) Wu, Y.; Breeze, M. I.; Clarkson, G. J.; Millange, F.; O'Hare, D.; Walton, R. I. Exchange of Coordinated Solvent during Crystallization of a Metal-Organic Framework Observed by in Situ High-Energy X-Ray Diffraction. *Angew. Chem., Int. Ed.* **2016**, *55*, 4992−4996.

(17) Yeung, H. H. M.; Wu, Y.; Henke, S.; Cheetham, A. K.; O'Hare, D.; Walton, R. I. In-Situ Observation of Successive Crystallizations and Metastable Intermediates in the Formation of Metal-Organic Frameworks. *Angew. Chem., Int. Ed.* **2016**, *55*, 2012−2016.

(18) Playford, H. Y.; Hannon, A. C.; Barney, E. R.; Walton, R. I. Structures of Uncharacterised Polymorphs of Gallium Oxide from Total Neutron Diffraction. *Chem. - Eur. J.* **2013**, *19*, 2803−2813.

(19) Kim, S.-W.; Iwamoto, S.; Inoue, M. Solvothermal Oxidation of Gallium Metal. *Ceram. Int.* **2009**, *35*, 1603−1609.

(20) Playford, H. Y.; Hannon, A. C.; Tucker, M. G.; Lees, M. R.; Walton, R. I. Total Neutron Scattering Investigation of the Structure of a Cobalt Gallium Oxide Spinel Prepared by Solvothermal Oxidation of Gallium Metal. *J. Phys.: Condens. Matter* **2013**, *25*, 454212.

(21) Nakatsuka, A.; Ikeda, Y.; Nakayama, N.; Mizota, T. Inversion Parameter of the $CoGa_2O_4$ Spinel Determined from Single-Crystal X-Ray Data. *Acta Crystallogr., Sect. E: Struct. Rep. Online* **2006**, *62*, i109−i111.

(22) Leccabue, F.; Pelosi, C.; Agostinelli, E.; Fares, V.; Fiorani, D.; Paparazzo, E. Crystal Growth, Thermodynamical and Structural Study of Cobalt Gallate ($CoGa_2O_4$) and Zinc Chromite ($ZnCr_2O_4$) Single Crystals. *J. Cryst. Growth* **1986**, *79*, 410−416.

(23) Moorhouse, S. J.; Vranjes, N.; Jupe, A.; Drakopoulos, M.; O'Hare, D. The Oxford-Diamond in Situ Cell for Studying Chemical Reactions Using Time-Resolved X-Ray Diffraction. *Rev. Sci. Instrum.* **2012**, *83*, 084101.

(24) Drakopoulos, M.; Connolley, T.; Reinhard, C.; Atwood, R.; Magdysyuk, O.; Vo, N.; Hart, M.; Connor, L.; Humphreys, B.; Howell, G.; et al. I12: The Joint Engineering, Environment and Processing (JEEP) Beamline at Diamond Light Source. *J. Synchrotron Radiat.* **2015**, *22*, 828−838.

DOI: 10.1021/acs.chemmater.7b01761
Chem. Mater. 2017, 29, 5053−5057

(25) Amundsen, T. G.; Øi, L. E.; Eimer, D. A. Density and Viscosity of Monoethanolamine + Water + Carbon Dioxide from (25 to 80) °C. *J. Chem. Eng. Data* **2009**, *54*, 3096−3100.
(26) Manohara, G. V.; Vishnu Kamath, P. Synthesis and Structure Refinement of Layered Double Hydroxides of Co, Mg and Ni with Ga. *Bull. Mater. Sci.* **2010**, *33*, 325−331.
(27) Radha, A. V.; Thomas, G. S.; Kamath, P. V.; Shivakumara, C. Suppression of Spinel Formation to Induce Reversible Thermal Behavior in the Layered Double Hydroxides (LDHs) of Co with Al, Fe, Ga, and In. *J. Phys. Chem. B* **2007**, *111*, 3384−3390.
(28) Arizaga, G. G. C.; Satyanarayana, K. G.; Wypych, F. Layered Hydroxide Salts: Synthesis, Properties and Potential Applications. *Solid State Ionics* **2007**, *178*, 1143−1162.
(29) He, J.; Wei, M.; Li, B.; Kang, Y.; Evans, D. G.; Duan, X. Preparation of Layered Double Hydroxides. *Layer. Double Hydroxides* **2006**, *119*, 89−119.
(30) Thevenot, F.; Szymanski, R.; Chaumette, P.; Fran, I.; Prrau, A. D. B.; Cedex, R. Preparation and Characterization of Al-Rich Zn Hydrotalcite-like Compounds. *Clays Clay Miner.* **1989**, *37*, 396−402.
(31) Xiao, Y. Q.; Thorpe, M. F.; Parkinson, J. B. Two-Dimensional Discrete Coulomb Alloy. *Phys. Rev. B: Condens. Matter Mater. Phys.* **1999**, *59*, 277−285.
(32) Evans, D. G.; Slade, R. C. T. Structural Aspects of Layered Double Hydroxides. *Struct. Bonding (Berlin)* **2005**, *119*, 1−87.
(33) Ruby, C.; Abdelmoula, M.; Naille, S.; Renard, A.; Khare, V.; Ona-Nguema, G.; Morin, G.; Génin, J. M. R. Oxidation Modes and Thermodynamics of FeII-III Oxyhydroxycarbonate Green Rust: Dissolution-Precipitation versus in Situ Deprotonation. *Geochim. Cosmochim. Acta* **2010**, *74*, 953−966.
(34) Richardson, I. G. Clarification of Possible Ordered Distributions of Trivalent Cations in Layered Double Hydroxides and an Explanation for the Observed Variation in the Lower Solid-Solution Limit. *Acta Crystallogr., Sect. B: Struct. Sci., Cryst. Eng. Mater.* **2013**, *69*, 629−633.
(35) Millange, F.; Walton, R. I.; O'Hare, D. O. Time-Resolved in Situ X-Ray Diffraction Study of the Liquid-Phase Reconstruction of Mg-Al-Carbonate Hydrotalcite-like Compounds. *J. Mater. Chem.* **2000**, *10*, 1713−1720.
(36) Pawley, G. S. Unit-Cell Refinement from Powder Diffraction Scans. *J. Appl. Crystallogr.* **1981**, *14*, 357−361.
(37) Xu, Z. P.; Zeng, H. C. Decomposition Pathways of Hydrotalcite-like Compounds $Mg_{1-x}Al_x(OH)_2(NO_3)_x{\cdot}nH_2O$ as a Continuous Function of Nitrate Anions. *Chem. Mater.* **2001**, *13*, 4564−4572.
(38) Evangelisti, F.; Moré, R.; Hodel, F.; Luber, S.; Patzke, G. R. 3d−4f $\{Co^{II}_3Ln(OR)_4\}$ Cubanes as Bio-Inspired Water Oxidation Catalysts. *J. Am. Chem. Soc.* **2015**, *137*, 11076−11084.
(39) Liu, H.; Moré, R.; Grundmann, H.; Cui, C.; Erni, R.; Patzke, G. R. Promoting Photochemical Water Oxidation with Metallic Band Structures. *J. Am. Chem. Soc.* **2016**, *138*, 1527−1535.
(40) Lutterman, D. A.; Surendranath, Y.; Nocera, D. G. A Self-Healing Oxygen-Evolving Catalyst. *J. Am. Chem. Soc.* **2009**, *131*, 3838−3839.
(41) Surendranath, Y.; Kanan, M. W.; Nocera, D. G. Mechanistic Studies of the Oxygen Evolution Reaction by a Cobalt-Phosphate Catalyst at Neutral pH. *J. Am. Chem. Soc.* **2010**, *132*, 16501−16509.
(42) Kanezaki, E. Thermal Behavior of the Hydrotalcite-like Layered Structure of Mg and Al-Layered Double Hydroxides with Interlayer Carbonate by Means of in Situ Powder HTXRD and DTA/TG. *Solid State Ionics* **1998**, *106*, 279−284.
(43) Rives, V. Characterisation of Layered Double Hydroxides and Their Decomposition Products. *Mater. Chem. Phys.* **2002**, *75*, 19−25.
(44) Thomas, G. S.; Kamath, P. V. Reversible Thermal Behavior of the Layered Double Hydroxides (LDHs) of Mg with Ga and in. *Mater. Res. Bull.* **2005**, *40*, 671−681.

DOI: 10.1021/acs.chemmater.7b01761
Chem. Mater. 2017, 29, 5053−5057